DINAME 2017 - Proceedings of the XVII International Symposium on Dynamic Problems of Mechanics
A. T. Fleury, D. A. Rade, P. R. G. Kurka (Editors), ABCM, São Sebastião, SP, Brazil, March 5-10, 2017

NONLINEAR DYNAMICS OF A SELF-FOLDING STRUCTURE ACTUATED BY SMA

Larissa Maciel da Fonseca[1], **Marcelo Amorim Savi**[1], **Alberto Paiva**[2]

[1] Universidade Federal do Rio de Janeiro - COPPE - Department of Mechanical Engineering
Center for Nonlinear Mechanics - MECANON - Technology Center - Rio de Janeiro - RJ - Brazil - 21.941.972,
larissamaciel.lah@gmail.com, savi@mecanica.coppe.ufrj.br

[2] Universidade Federal Fluminense - Volta Redonda School of Engineering - Department of Mechanical Engineering 420 Trabalhadores Av. - Volta Redonda - RJ - Brazil - 27.255-125 , paiva.ufrj@gmail.com

Abstract: Origami, the ancient Japanese art of paper folding, creates a sculpture representation through pattern folds of a flat paper sheet producing a desired shape. Origami-based structures have been increasingly investigated and applied in various fields of knowledge. The majority of these applications are motivated by adaptive and compacting capacities. The use of smart materials is an important issue for actuation of origami systems. Shape memory alloys (SMAs) and magnetic materials are of special interest due to their capacity to generate forces and displacements. Since origami systems are slender structures, they are usually close to stability limits with important dynamical issues to be investigated. In this paper, a dynamical investigation of an origami structure called "origami-ball" actuated by shape memory alloys elements are carried out. It is proposed a one-degree of freedom oscillator to represent the origami-ball dynamics based on geometric analysis and symmetry assumptions. A constitutive model with internal constraints is employed to describe the thermomechanical behavior of the SMA actuator. The system has constitutive and geometric nonlinearity presenting rich and complex responses. Numerical simulations treat different conditions associated with external stimuli, considering thermal and mechanical loads. Results show periodic and irregular responses. Situations where inputs can change the expected operation of the origami are highlighted.

Keywords: Smart Structures, Origami System, Nonlinear Dynamic, Shape Memory Alloy, Self-Foldable Systems

INTRODUCTION

Origami has the unique feature to create three-dimensional structures from two-dimensional materials. This remarkable characteristic has attracted attention from various fields such as education (Andreass, 2011) and mathematics (Alperin, 2000; Glassner, 1996). Recently, the Japanese art has inspired engineering in the development of new structures that are already employed in architecture and decorations, due to the beauty of the generated forms. Applications on robotics, bioengineering and aerospace systems have great potential. The combination of origami system with control elements can increase the application capacity providing smart systems with adaptive aspects. Morphing and movements are the main motivation of these systems. Shape memory alloys (SMAs) and magnetic materials are of special interest to be used as actuators in this kind of system.

Origami systems with SMA actuators have been proposed for different purposes. Minimally invasive surgery is investigated by Zhang et al. (2014) using a 4 degrees of freedom system. Stents constructed from the fold of a single NiTi alloy sheet is proposed by Kuribayashi (2006). A folding wheel driven by SMAs is another application for robotics. The thermal control enables to change its diameter, adapting to different environments (Lee *et al*., 2013).

Origami wheel actuated by SMA actuators is an interesting approach for robots that need to deal with irregular soil and obstacles. The idea is to alter the origami wheel between different configurations, changing the robot performance. SMA are employed to provide self-folding capacity that can be induced by temperature changes.

Origami systems have been analyzed by different perspectives. Geometrical analysis is of great importance (Tachi, 2010; Buri and Weinand, 2008). Quasi-static analysis of the configuration changes is another important analysis found in literature (Turner, 2015). Finite element method is usually employed in order to obtain a proper comprehension of the involved phenomena (Gilewski *et al*., 2014; Lv *et al*., 2014). Only few articles are dedicated to dynamical analysis.

Dynamical systems with SMA elements are usually associated with complex reponses. Savi (2015) presents a review of dynamic applications of shape memory systems that includes oscillators, adaptive vibration absorbers, rotary systems and adaptive structures.

This work deals with a dynamical investigation of an SMA-origami system called origami-ball employd for robotic applications. A mathematical model is developed considering a single degree of freedom equivalent system that describes the dynamical behavior of the origami-ball. The thermomechanical behavior of SMAs is described by the constitutive model proposed by Paiva and Savi (2006). The origami system has constitutive and geometrical nonlinearities.

The paper is organized as follows: Initially, SMA constitutive equations are presented. Afterward, the origami system is investigated proposing a single degree of freedom system to describe the nonlinear dynamics. Numerical simulations are then carried out to simulate several operational conditions, represented by external issues. Finally, conclusion remarks are presented.

CONSTITUTIVE MODEL

There are many possibilities to describe SMA thermomechanical behavior (Paiva and Savi, 2006; Lagoudas, 2012). One of these possibilities can be classified as models with internal constraints. Paiva and Savi (2006) proposed a model that has four macroscopic phases represented by volume fractions: β_1 associated with tension detwinned martensite (M^+); β_2 associated with compression detwinned martensite M^-); β_3 associated with the austenitic phase (A); and β_4 related temperature induced martensite (M). In this work, we consider a simplified version of the one-dimensional model, neglecting plasticity, tension/compression asymmetry and TRIP effect. The model is developed by following the generalized standard materials formalism, being thermodynamically consistent. It is proposed a Helmholtz free energy density potential for each one of the phases as a function of observable state variables: elastic strain, ε_e, and temperature, T. Afterward, it is defined a mixture free energy, Ψ, and a dissipation potential, Φ. Paiva and Savi (2006) presented details about the formulation of the model that is represented by the following equation.

$$\sigma = E\varepsilon + (\alpha + E\alpha_h)(\beta_2 - \beta_1) - \Theta(T - T_0) \tag{1}$$

$$\dot{\beta}_1 = \frac{1}{\eta_1}\left\{\alpha\varepsilon + \Lambda_1 + \left(2\alpha_h\alpha + E\alpha_h^2\right)(\beta_2 - \beta_1) + \alpha_h\left[E\varepsilon - \Theta(T - T_0)\right] - \partial_{\beta_1} J_\pi\right\} - \partial_{\dot{\beta}_1} J_\chi \tag{2}$$

$$\dot{\beta}_2 = \frac{1}{\eta_2}\left\{\alpha\varepsilon + \Lambda_1 + \left(2\alpha_h\alpha + E\alpha_h^2\right)(\beta_2 - \beta_1) + \alpha_h\left[E\varepsilon - \Theta(T - T_0)\right] - \partial_{\beta_2} J_\pi\right\} - \partial_{\dot{\beta}_2} J_\chi \tag{3}$$

$$\dot{\beta}_3 = \frac{1}{\eta_3}\left\{-\frac{1}{2}(E_A - E_M)\left[\varepsilon + \alpha_h(\beta_2 - \beta_1)\right]^2 + \Lambda_3 + (\Theta_A - \Theta_M)(T - T_0)\left[\varepsilon + \alpha_h(\beta_2 - \beta_1)\right] - \partial_{\beta_3} J_\pi\right\} - \partial_{\dot{\beta}_3} J_\chi \tag{4}$$

where E is the elastic modulus and Θ is the thermal expansion coefficient, α is the phase transformation coefficient and α_h deals with the hysteresis loop width; T_0 is a reference temperature at which the SMA has no strain. The parameters E and Θ are defined by rule of mixture given by $E = E_M - \beta_3(E_M - E_A)$ and $\Theta = \Theta_M - \beta_3(\Theta_M - \Theta_A)$, respectively. The functions Λ_A e Λ_M define the critical phase transformation stress, being temperature dependent. Parameters η_A and η_M define the intrinsic dissipation of the material and can assume different values for loading or unloading processes. Constraints related to phase coexistence are described by a convex set π, Eq. (5). Geometrically, this set is related to a tetrahedron showed in Fig. 1. $J_\pi(\beta_i)$ is the indicatrix function of the convex set π, and states the restrictions associated to the phase coexistence.

$$\pi = \{\beta_i \in \Re | 0 \leq \beta_i \leq 1; \beta_1 + \beta_2 + \beta_3 \leq 1\} \tag{5}$$

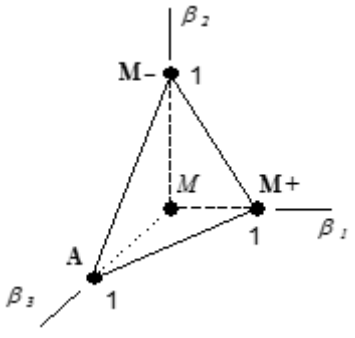

Figure 1 – Geometric representation of coexistence phases restrictions.

Another convex set χ deals with other constraints related to phase transformations.$J_\chi(\dot{\beta}_i)$ is indicatrix function associated with the convex and represents the subdiferential of these functions. Note that subdifferential definitions are equivalent to a projection to the convex set and can be replaced by Lagrange multipliers.

Oliveira *et al*. (2016) developed a three-dimensional version of the proposed model. Based on that, it is possible to use similar mathematical model in order to describe torsion behavior by changing the normal stress σ for the shear one τ, the normal strain ε by the shear one γ and the elastic moduli E by the shear moduli G. The portion related to thermal expansion $(\Theta(T - T_0))$ is neglected because its magnitude order is smaller than the other terms.

The numerical procedure to solve the constitutive equations Eq. (1) to Eq. (5) is based on operator split technique (Ortiz *et al*., 1983). Subdiferentials are treated separately from the resolution of the volume fractions differential equations, by

using the implicit Euler method. If the calculated values do not meet the constraints represented by Fig. 1, orthogonal projections are performed. For details, please see Paiva and Savi (2006).

SMA helical springs can be described by similar equations that represent force-displacement curves. The essential hypothesis for this is that phase transformation is homogeneous through the spring wire cross section. See Aguiar *et al*. (2010) and Enemark *et al*. (2016) for details. Thus, SMA force-displacement curve is given by Eq. (6).

$$F_{SMA} = \left(\frac{\pi d^3}{6D}\right)_{SMA} \left[G \left(\frac{d}{\pi D^2 N}\right)_{SMA} u + (\alpha + G\alpha_h)(\beta_2 - \beta_1) \right] \tag{6}$$

ORIGAMI-BALL

The origami-ball is built using the waterbomb pattern. The origami-ball has large applicability (Martinez, 2012; Onal *et al*., 2011) being interesting due to its peculiar characteristic of changing its shape and size. The forthcoming analysis establishes geometrical relations of the origami-ball that is essentially based on symmetry hypothesis. Under this assumption, unitary square cells are equal presenting equal deformations (Lee *et al*., 2013). Besides, origami has rigid panels and folding occurs only on the creases. Figure 2 presents the origami system composed by the origami base, SMA actuators (Actuator 1), an elastic passive spring (Actuator 2) and 2 octagonal acrylic plates at the ends.

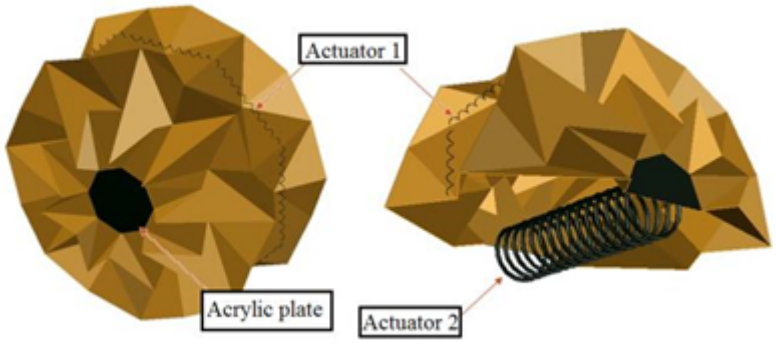

Figure 2 – Origami structure, with the actuators 1 (SMA element) and 2 (elastic passive spring) and the acrylic plates.

The unitary cells are squares with size $2l$ and the acrylic plate has a limited circumference of radii l_p. The actuator 1, which length is L_1, is responsible for closing the structure while actuator 2, which half-length is L_2, is responsible for the restoring force. By using the symmetry hypothesis, is possible to describe the structure geometry just by analyzing two plans: circumferential (XZ) and longitudinal (YZ), represented at Fig. 3(b). The unitary cell, which behavior is assumed to be equal at all the structure, is represented at Fig. 3(a)

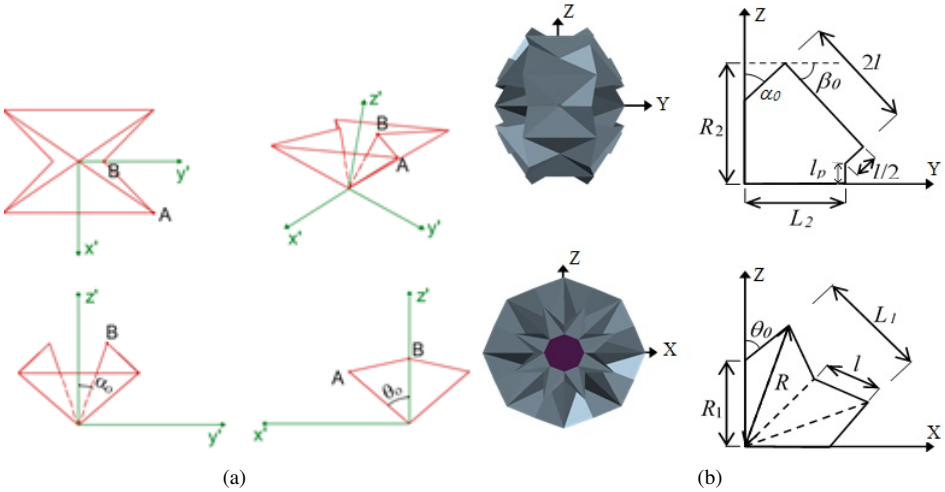

Figure 3 – (a) Unitary cell of the origami base; (b) Longitudinal (YZ) and circumferential (XZ) plan views.

By performing proper projections on the axes shown in Fig. 3(b), it is possible to obtain geometric relations for the origami. Equation (7) comes from the unitary cell, being described in the local variables by taking the distance between the points A and B, once that $\|\overline{AB}\|=l$. Equations (8) and (9) are obtained from plan YZ and Eq. (10) to (13) come from the circumferential view. Equations (7) to (12) are essentials to define the geometric relation of the origami structure, while Eq. (13) is an additional relation that is important to describe the dynamical behavior of the system.

$$cos\theta_0 cos\alpha_0 + sin\alpha_0 = 1 \tag{7}$$

$$L_2 = lsin\alpha_0 + 2lcos\beta_0 - \frac{l}{2}sin\beta_0 \tag{8}$$

$$R_2 = l_p + 2lsin\beta_0 + \frac{l}{2}cos\beta_0 \tag{9}$$

$$R_2 - R_1 = lcos\alpha_0 \tag{10}$$

$$L_1 = 2lsin\theta_0 \tag{11}$$

$$R_1 = lsin\left(\theta_0 - {}^{\pi}/_{8}\right)/sin{}^{\pi}/_{8} \tag{12}$$

$$R = L_1\sqrt{2 + {}^{\sqrt{2}}/_{2}} \tag{13}$$

The system composed by Eq. (7) to Eq. (12) is solved analytically, leading to an explicit relation between the actuators' length L_1 and L_2, $L_2 = f(L_1)$, remembering that L_2 corresponds to the half-length of the actuator 2. It is assumed that l = 0.065m and l_p = 0.04 m; due to physical restrictions, the structure has boundaries that can be represented by the range $L_1 \in [0.0555.0.1225]m$.

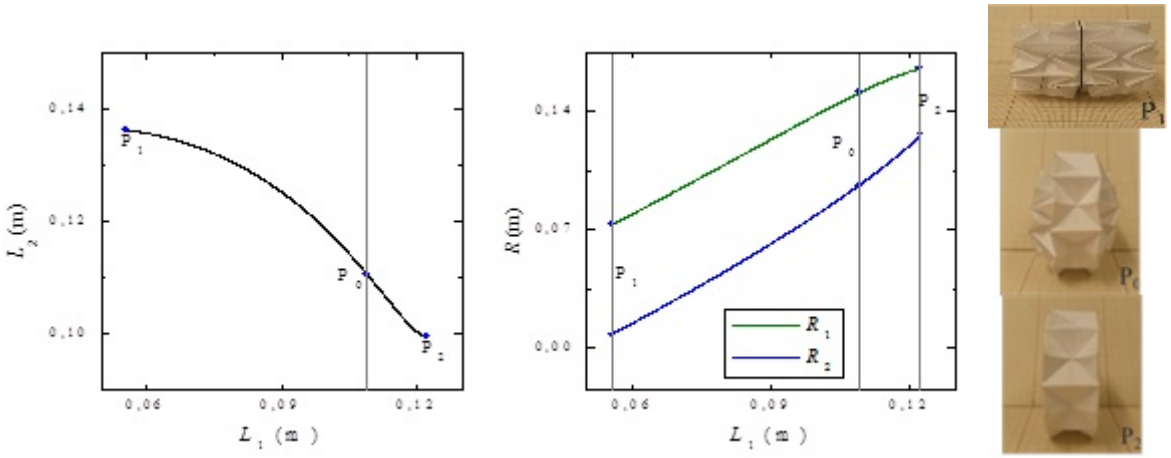

Figure 4 – Geometric relations of the origami structure and configurations. (a) Relation $L_2 = f(L_1)$; (b) Radii variation. P_2: Flat circular tube; P_0: Initial configuration; P_1: Circular tube.

Static and dynamic equations

Equilibrium considerations is now of concern assuming symmetry hypothesis. Based on that, one can obtain the reaction (E_1), on plan XZ, from the application of a force (E_2) applied on plan YZ (Fig. 5). By assuming that the force E_2 is homogeneously distributed through the structure, it generates a correspondent force E_1 on the other plan. The relation between them is purely geometric, being given by.

$$E_1 = E_2\frac{cos\alpha_0 + \sqrt{2}cos\theta_0}{4cos\beta_0} \tag{14}$$

The origami system has a complex behavior with tridimensional movements described by nonlinear relations. Notwithstanding these movements are coupled allowing a simplification of the general description. The origami base has a mass $8m$ that is assumed discretely disposed around the circumferential plan in such a way that each mass m is associated with one SMA actuator L_1. Furthermore, each acrylic plate has mass M, associated with L_2. Spring displacements are written as $u_E = L_2 - L_2^0$ (actuator 2) and $u = L_1 - L_1^0$ (actuator 1), where superscript "0" is related to the reference configuration (P_0). Dynamic balance considers masses m and M. Mass M is treated on longitudinal plan view, Y direction; mass m is treated on the circumferential plan view, radial direction. A linear viscous dissipation is considered on the equation and is related to dissiptaions due to the folding process. Moreover, elastic spring force, F_E, is given by,Eq. (15), where $L_2 = f(L_1)$ presented in Fig. 4 can be rewritten in terms of displacements. External forces can be applied both to the acrylic plates (mechanical efforts) or the SMA spring conectors (mechanical or termal loads). This paper takes into account only thermal loads applied on the SMA spring and the mechanical loads applied on the acrylic plates. So, the equation takes into account the decoposition of the external force on the circumferential plane.

$$F_E = \left(\frac{Gd^4}{6D^3N}\right)_E f(u) \tag{15}$$

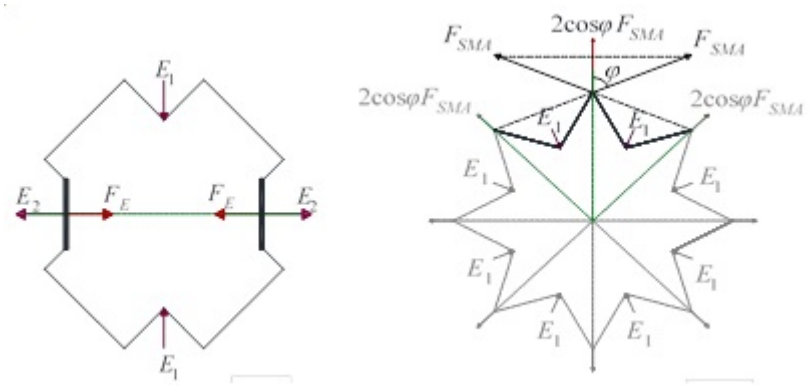

(a) (b)

Figure 5 – Free body diagram at longitudinal (a) and circumferential (b) plan views.

Under these assumptions, the following equations of motion are obtained.

$$\begin{cases} M\ddot{u}_E + F_E = E_2 + F(\tau) \\ m\ddot{r} + \sqrt{2}F_{SMA} + c\dot{u} = E_1 cos^{\pi}/_8 \end{cases} \tag{16}$$

where r is the variation of the length R and is given by

$$r = (L_1 - L_1^0)\sqrt{\frac{2+\sqrt{2}}{2}} \tag{17}$$

By assuming that $\ddot{f} = f_1(u)\ddot{u} + f_2(u)\dot{u}^2$, it is possible to write:

$$\ddot{u}_E = f_1(u)\ddot{u} + f_2(u)\dot{u}^2 \tag{18}$$

Since forces E_1 and E_2 are coupled (Eq. (14)), equations of motion can be rewritten as a single degree of freedom system. Based on that, the dimensionless equation of motion is presented in the sequence.

$$\begin{cases} u' = v \\ v' = \frac{\delta(\tau)+\gamma u+(\overline{\alpha}+\overline{\alpha}_h)(\beta_2-\beta_1)-\kappa f-\overline{m}v^2 f_2 h+\xi v}{\overline{m}f_1 h-\sqrt{2+\sqrt{2}}/_2} \end{cases} \tag{19}$$

where the following parameters are employed

$$\begin{gathered} \lambda = \frac{1}{m\omega_0^2}\left(\frac{d^6 G}{6\pi N^3 D^7}\right)_{SMA}; \overline{\alpha} = \frac{\alpha}{m\omega_0^2}\left(\frac{\pi d^3}{6D}\right)_{SMA}; \overline{\alpha}_h = \frac{\alpha_h}{m\omega_0^2}\left(\frac{\pi d^3 G}{6D}\right)_{SMA}; \overline{m} = \frac{M}{m}; \\ \kappa = \frac{1}{m\omega_0^2}\left(\frac{Gd^4}{6D^3 N}\right)_E; h = \frac{cos\frac{\pi}{8}(cos\alpha_0+\sqrt{2}cos\theta_0)}{4cos\beta_0} \end{gathered} \tag{20}$$

Note that these parameters are related to the constitutive model $(\lambda, \overline{\alpha}, \overline{\alpha}_h)$, the stiffness of the passive elastic spring,κ, and with geometric assumptions,h. Besides, dimensionless time τ is considered and $()' = d()/d\tau$, where ω_0 is related to the natural frequency of a 1DOF SMA oscillator of cross section area A_{SMA} and length L.

$$\omega_0 = \sqrt{\frac{G_M A_{SMA}}{mL}} \tag{21}$$

Numerical Simulations

This section presents numerical simulations of the origami system considering different operational conditions. Different thermomechanical loads are assumed for this aim. Table 1 presents system parameters employed for all simulations.

Table 1 – System parameters.

α (MPa)	α_h	G_A (GPa)	G_M (GPa)	L_0 (MPa)	L (MPa)	L_A (MPa)
260	0.048	54	42	0.15	41.5	0.63
L_0^A (MPa)	η^C (MPa.s)	η^D (MPa.s)	η_A^C (MPa.s)	η_A^D (MPa.s)	m (kg)	M (kg)
185	10	27	10	27	0.04	0.12
d_{SMA} (m)	D_{SMA} (m)	N_{SMA}	d_E (m)	D_E (m)	N_E	G_E (GPa)
2.0×10^{-3}	4.8×10^{-3}	10	2.0×10^{-3}	20.0×10^{-3}	30	80

Free vibrations

Initially, free vibration analysis is carried out, exploring the equilibrium point structure and their temperature dependent behavior. This analysis is performed assuming that external forces vanish. Figure. 6 shows phase portraits for a viscous dissipation $\xi = 0.05$ and three different temperatures: $T = 288K$ (low temperature where martensite is stable is a stress-free state); $T = 290K$ (intermediate temperature where both austenite and martensite are stable); $T = 310K$ (high temperature where austenite is stable in the absence of strain). Note that the system presents five equilibrium points at low temperature (Fig. 6a). The same occurs for intermediate temperature (Fig. 6b and c). For high temperature, only one equilibrium point is observed (Fig. 6d). These points are defined from the phase transformations being close related to the stable phase. Steady state is related to M^+, M, and M^- for low and intermediate temperatures while high temperature is associated with phase A. Geometrical nonlinearities alter the general structure of the equilibrium points. It is important to observe that for the intermediate temperature case M phase is restricted to a small range of phase space.

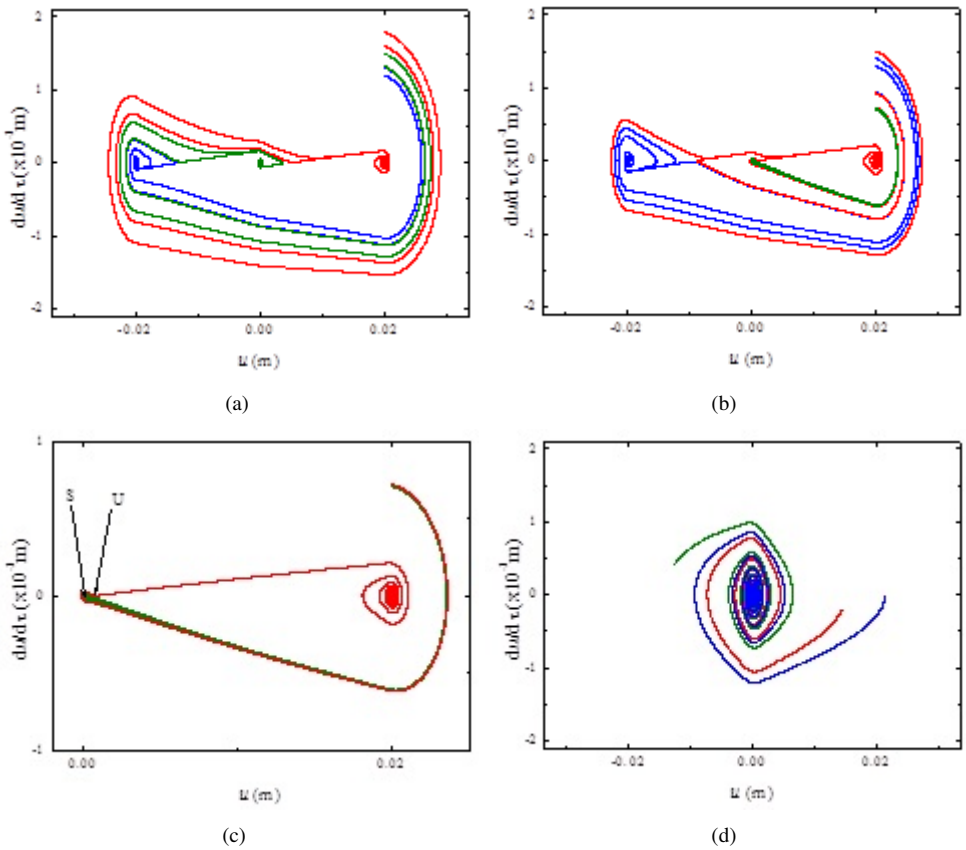

Figure 6 – Phase portraits for different temperatures. (a) T=288K; (b) T=290 K; (c) Zoom at (b); (d) T=310 K.

The influence of thermal loading rate is now of concern. The connection between material temperature and loading rate was initially identified by Mukherjee *et al*. (1985) in experimental procedures. This behavior is associated with rate dependent behavior of SMAs, close related to thermal processes that occur during the phase transformation. In brief, it is important to highlight that austenite-martensite phase transformation is exothermic, while the reverse transformation is endothermic. High loading rates alter heat transfer to environment raising the temperature of the alloy (Ozbulut and Hurlebaus, 2010). The thermomechanical description of the loading rate dependence needs to consider energy equation including thermomechanical coupling terms. Monteiro Jr. *et al*. (2007) discussed details about thermomechanical couplings showing that it can be described by a viscous effect on the constitutive model. The constitutive model of Paiva *et al*. (2005) employed in this work is able to describe this effect.

Hence, consider a damped system with ξ=0.05, subjected to two different thermal cycles (Fig. 7a): the first (red curve) considers that the cooling rate is about 25% of the heating rate; the second (green curve), about 12.5%. It is observed that in the first case, the system stabilizes at M^+ (Fig. 7b, e, h). For the second case, the system dissipates more energy, stabilizing at M phase (Fig. 7c, f, i).

A third case is treated considering the second thermal cycle but changing the dissipation coefficient for ξ = 0.01. Under this new condition, the system stabilizes in a different point (Fig. 7d). The reduction of the dissipation causes a situation where the system dissipates less energy for the same period of time and the same thermal cycle. Thus, after cooling, origami has energy greater than that contained in the M stability region, leading to accomplish the complete transformation and stabilize at M^+ (Fig. 7g, j). This is associated with the open configuration of the origami. By raising the dissipation or cooling rate, it is possible to maintain the origami-ball semi-opened.

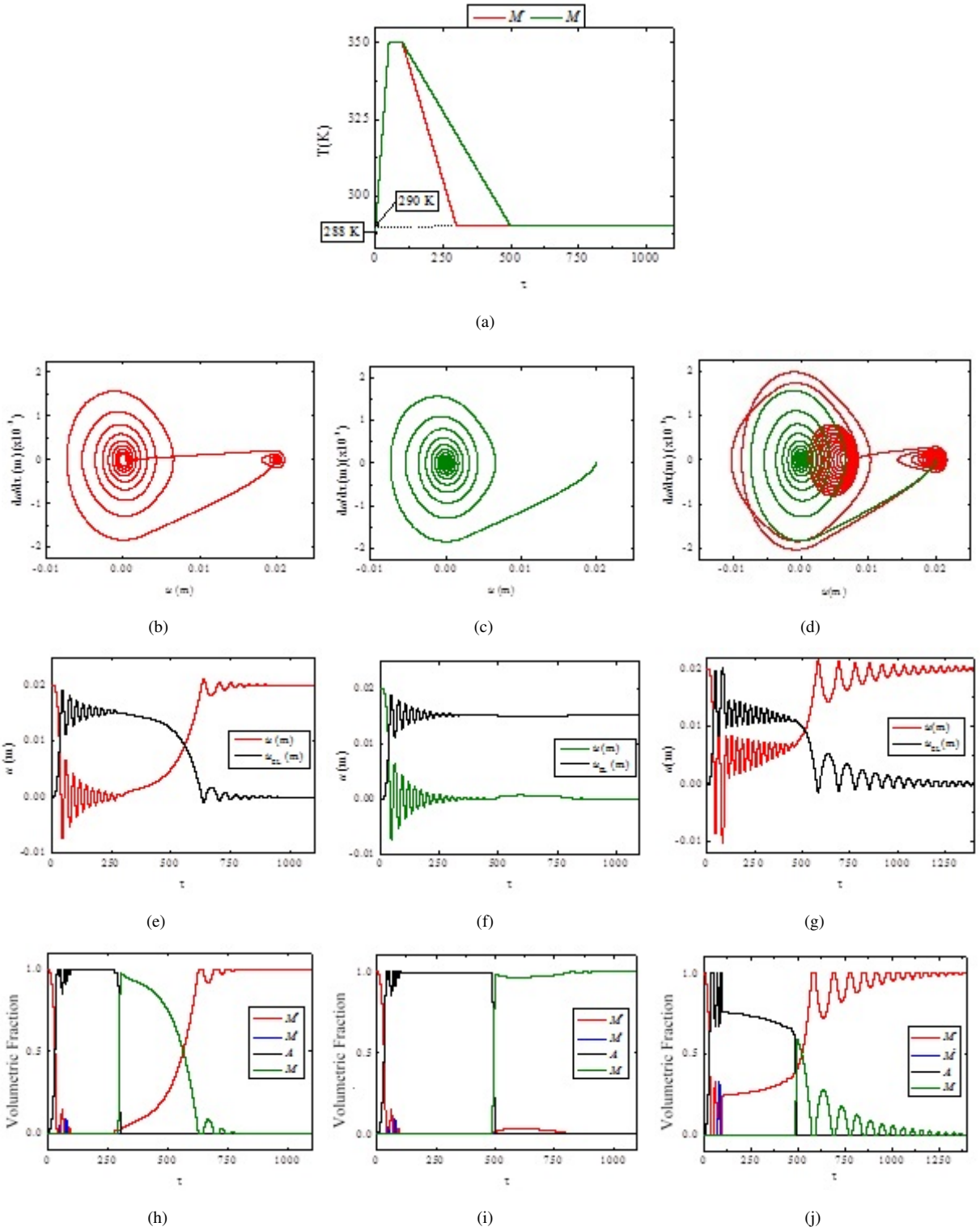

(a)

(b) (c) (d)

(e) (f) (g)

(h) (i) (j)

Figure 7 – System stabilization for different rates and dumping coefficients. (a) Thermal load. (b) to (d) Phase portraits. (e) to (g) Springs displacements on time. (h) to (j) Volumetric fractions evolution.

Mechanical loads - Forced vibration

Forced vibration analysis is now carried out, exploring the sensitivity of the system to different mechanical loads, and its temperature dependence. The analysis considers two different excitations: square wave (Eq. (24)) and sawtooth wave (Eq. (25)), as its expansions as Fourier series. All these forces have period p and amplitude δ. All excitations are applied trying to close the origami structure, hence they are presented as negative forces.

$$F(\tau) = \frac{\delta}{2} - \frac{2\delta}{\pi} \sum_{n=1}^{800} \frac{1}{2n-1} sin\left(\frac{2(2n-1)\pi\tau}{p}\right) \tag{22}$$

$$F(\tau) = \frac{\delta}{2} - \frac{\delta}{\pi}\sum_{n=1}^{800}\frac{1}{n}sin\left(\frac{2n\pi\tau}{p}\right) \tag{23}$$

Figure 8 shows the Poincaré sections for sawtooth wave (Fig. 8a), with δ=10^{-5},p=20 and T=288 K, and square wave (Fig. 8d), with δ=10^{-5}, p=10 and T=290 K. Poincaré sections (Fig. 8b and e) show a strange attractor like structure related to a chaotic response. By heating the SMA, system behavior changes from chaotic-like to a period-2 response (Fig. 8c) in a sawtooth wave external force system, and to a period-4 response (Fig. 8f), in a square wave external force system.

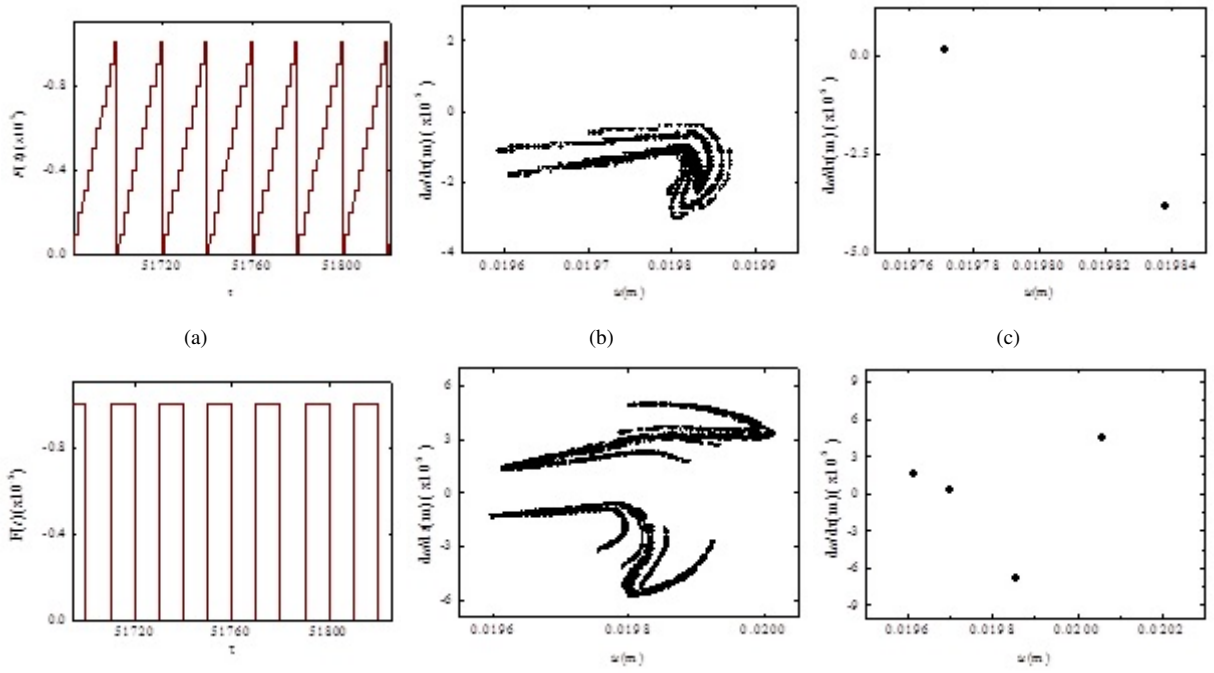

Figure 8 – Origami-ball response to mechanical loads. (a) Sawtooth wave. (b) Poincaré section for chaotic-like response. (c) State subspace and Poincaré section for period-2 response for T=290 K. (d) Square wave. (e) Poincaré section for chaotic-like response. (f) State subspace and Poincaré section for period-4 response for T=292 K.

CONCLUDING REMARKS

This paper proposes a single-degree of freedom oscillator to represent the complex nonlinear behavior of the SMA origami-ball system. SMA themomechanical behavior is described by a constitutive model with internal constraints. Numerical simulations explore free and forced vibrations. Free vibration analysis explores the equilibrium point structure and its temperature dependent behavior. Rate dependent behavior can provide different responses and final configurations for distinct loading rates. Thermal loads can promote the opening or the shutdown of the system, depending on the heating/cooling rate and the system dissipation. Force vibration analysis considers different types of periodic excitations. Complex behavior is expected and special attention is dedicated to chaos. It is observed that the SMA heating can change the structure behavior from a chaotic-like response to a periodic motion.

REFERENCES

Aguiar, R. A. A., Savi, M. A., Pacheco, P. M. C. L., 2010, Experimental and numerical investigations of shape memory alloy helical springs. Smart Materials and Structures 19(2): 025008.

Alperin, R.C., 2000, A Mathematical Theory of Origami Constructions and Numbers, New York Journal of Mathematics, Vol. 6, pp. 119-133

Andreass, B., 2011, Origami art as a means of facilitating learning, Procedia - Social and Behavioral Sciences, Vol. 11, pp. 32-36, ISSN 1877-0428, http://dx.doi.org/10.1016/j.sbspro.2011.01.028

Buri, H., Weinand, Y., 2008, ORIGAMI – Folded Plate Structures, Architecture, 10th World Conference on Timber Engineering, Miyazaki, Japan, 2-5.

Gilewski, W., Pelczynski, J., Stawarz, P., 2014, A Comparative Study of Origami Inspired Folded Plates, XXIII R-S-P seminar, Theoretical Foundation of Civil Engineering, pp. 220-225.

Glassner, A., 1996, More Origami Solids, vol. 16, no. 5, September 1996, pp. 85-91.

Kuribayashi K., Tsuchiya K., You Z. *et al*., 2006, Self-deployable origami stent grafts as a biomedical application of Ni-rich TiNi shape memory alloy foil, Mater Sci Eng: A, 419 (1), pp. 131–137

Lagoudas, D.C. (editor and co-author), 2008, Shape Memory Alloys: Modeling and Engineering Applications, Springer-Verlag.

Lee D. Y. *et al*., 2013, The Deformable Wheel Robot Using Magic-Ball Origami Structure, International Design Engineering Technical Conferences & Computers and Information in Engineering Conference, Portland, Oregon.

Lv, C., Krishnaraju, D., Konjevod, G., Yu, H., Jiang, H., 2014, Origami based Mechanical Metamaterials, Scientific Reports 4: 5979.

Martinez R.V., Fish C.R., Chen X. *et al*., 2012, Elastomeric Origami: Programmable Papper-Elastomer Composites as Pneumatic Actuators, Advanced Functional Materials.

Monteiro Jr., P. C. C., Savi, M. A., Netto, T. A., *et al*., 2007, On the Thermomechanical Coupling in Shape Memory Alloys, 19th International Congress of Mechanical Engineering, November 5-9, Brasilia.

Mukherjee, K., Sircar, S., Dahotre, N. B., (1985), "Thermal effects associated with stress-induced martensitic transformation in Ni-Ti alloy", Mater. Sci. Eng. 74, 75-84.

Oliveira, S. A., Savi, M. A., Zouain, N., 2016, A three-dimensional description of shape memory alloy thermomechanical behavior including plasticity, Vol. 38, Issue 5, pp. 1451–1472.

Onal C. D., Wood R. J. E Rus D., 2011, Towards printable robotics: origami-inspired planar fabrication of three-dimensional mechanisms, International Conference of Robotics and Automation, IEEE Int. Conf. (Piscataway, NJ: IEEE), pp 4608–13

Ortiz, M., Pinsky, P. M., Taylor, R. L., 1983, "Operator Split Methods for the Numerical Solution of the Elastoplastic Dynamic Problem", Computer Methods of Applied Mechanics and Engineering, 39: pp.137157.

Ozbulut, O.E., Hurlebaus, S., 2010, Neuro-fuzzy Modeling of Temperature- and Strain-rate-dependent Behavior of NiTi Shape Memory Alloys for Seismic Applications. Journal of Intelligent Material Systems and Structures, Vol. 21, No. 8, pp. 837-849.

Paiva A., Savi M.A., 2006, An overview of constitutive models for shape memory alloys, Mathematical Problems in Engineering, vol. 2006, Article ID 56876, pg. 30.

Savi, M. A., 2015, Nonlinear dynamics and chaos in shape memory alloy systems, International Journal of Non-Linear Mechanics, Vol. 70, pp. 2-19.

Tachi, T., 2010, Geometric Considerations for the Design of Rigid Origami Structures, Proceedings of IASS Symposium 2010, Shanghai, China, pp. 771-782.

Zhang K., Salerno M., Menciassi A., *et al*., 2014, A Novel 4-DOFs Origami Enabled, SMA Actuated, Robotic End-effector for Minimally Invasive Surgery, International Conference on Robotics & Automation (ICRA)

RESPONSIBILITY NOTICE

The authors are the only responsible for the material included in this paper.